Applied Physics Express **8**, 065503 (2015)
http://dx.doi.org/**10.7567/APEX.8.065503**

Improved efficiency of electrodeposited p-CuO/n-Cu_2O heterojunction solar cell

Charith Jayathilaka[1,2], Vassilios Kapaklis[3], Withana Siripala[2], and Sumedha Jayanetti[1*]

[1]*Department of Physics, University of Colombo, Colombo 3, Sri Lanka*
[2]*Department of Physics, University of Kelaniya, Kelaniya, Sri Lanka*
[3]*Department of Physics and Astronomy, Uppsala University, Box 516, S-75120 Uppsala, Sweden*
E-mail: sumedhajayanetti@gmail.com

Received May 14, 2015; accepted May 19, 2015; published online June 4, 2015

We report electrodeposition of n-type cuprous oxide (Cu_2O) films on p-type CuO films electrodeposited on Ti substrates for forming p-CuO/n-Cu_2O heterostructures. X-ray diffraction (XRD) and scanning electron microscopy (SEM) analysis revealed that the films had good structural quality, with substrates being well-covered by the films. The p-CuO/n-Cu_2O heterojunctions exhibited good photovoltaic properties and diode characteristics. The surfaces of Cu_2O films subject to ammonium sulfide treatment exhibited enhanced photocurrents. Under AM 1.5 illumniation, the obtained sulfur-treated and annealed Ti/p-CuO/n-Cu_2O/Au solar cell structure yielded energy conversion efficiency of 0.64%, with $V_{oc} = 220$ mV and $J_{sc} = 6.8$ mA cm^{-2}. © 2015 The Japan Society of Applied Physics

Photovoltaic devices have attracted increasing attention as a sustainable clean energy source. Among the materials being studied, photovoltaic devices based on oxide semiconductors are promising candidates for next-generation thin film solar cells, owing to their unique physical properties such as good adherence to substrates, hardness and stability.[1,2] Two of the semiconducting copper oxides, cuprous oxide (Cu_2O) and cupric oxide (CuO), are good potential candidates for solar cells and other applications.[3] These materials are especially suitable for high-efficiency solar cells because their optical band gaps, 1.21 to 2 eV (for CuO) and 1.8 to 2.5 eV (for Cu_2O), make these materials suitable for solar energy absorption.[3] The stability, low photo-degradation rates, abundance and non-toxicity of the copper oxides make them more advantageous for photovoltaic (PV) applications.[4] The theoretical power conversion efficiencies of Cu_2O and CuO are ~20% and ~30%, respectively.[5] The reported efficiencies for Cu_2O-based homojunction and heterojunction solar cell devices have remained around 2% until in a recent article by Minami et al. an efficiency of 6.1% was reported for an MgF_2/AZO/$(Ga_{0.975}Al_{0.025})_2O_3$/$Cu_2O$:Na heterojunction solar cell structure.[6,7] This indicates that Cu_2O is a promising material for commercially viable future photovoltaic device applications. On the other hand, CuO has rarely been reported as an active solar cell absorber in the literature. In one such case, CuO nanocrystals have been combined with an organic compound, to achieve the efficiency of 0.04%.[8] Photovoltaic effects have also been observed in core–shell CuO/C_{60} junctions with an estimated efficiency of 0.02%,[9] as well as in thin film heterojunctions of the same type, with efficiency on the order of 10^{-4}%.[10] It has been reported that ZnO/CuO heterojunctions and CuO nanowires covered with n-type ZnO have efficiencies on the order of 10^{-5}%[11] and nearly 0.1%,[12] respectively. Recently, the highest efficiency of 0.41% was reported for a p-CuO/n-Si heterostucture solar cell.[13] Unlike the homojunction structure, there is an internal crystal structure interface between two different materials in any heterojunction device; thus, the optical refractive index changes at the interface. Therefore, for heterojunction solar cell systems, for minimizing the reflectance it is preferable to use materials with similar refractive indices and to have a window layer with a larger refractive index than that of the absorption layer. The refractive indices of CuO and Cu_2O are $n = 2.58$ and $n = 3.1$, respectively, for the wavelength of 550 nm.[14] Therefore, CuO/Cu_2O heterojunction solar cell structures are ideal for high-efficiency solar cell systems. Several methods, such as thermal oxidation, chemical oxidation, anodic oxidation, vacuum evaporation, spin coating and electrodeposition have been used for preparation of Cu_2O and CuO thin films. Among these, electrodeposition is considered as a simpler and more convenient fabrication method. As a technique that does not require expensive equipment and allows achieving higher deposition rates at low processing temperatures, electrodeposition can be used for fabricating uniform films on various substrates of complex geometries.[15–17] The ability to control the conductivity type by using electrodeposition is especially important for fabrication of Cu_2O thin films, which are normally considered p-type materials. Reports on CuO/Cu_2O heterojunctions are very limited in the literature, owing to the difficulty associated with growing n-type Cu_2O (or CuO). Recently, considerable attention has been devoted to developing CuO/Cu_2O heterojunctions, after Siripala et al. reported the growth of n-type Cu_2O thin films by using electrodeposition.[18] Wijesundara et al. have reported fabrication of p-CuO/n-Cu_2O heterojunctions by annealing an electrodeposited Cu_2O thin film at 500 °C for 30 min for producing a p-CuO film and then electrodepositing an n-Cu_2O thin film on top of the former. However, the resulting p-CuO/n-Cu_2O heterojunction has yielded a low photocurrent of 310 μA cm^{-2}.[19] One known drawback of the electrodeposition method is high resistivity of the fabricated Cu_2O films. This has been attributed to the high density of defects that are inherent to the electrodeposited Cu_2O thin films, making it difficult to fabricate good-quality devices. Recently, we found that performing sulfur passivation by $(NH_4)_2S$ is very useful for modifying the surfaces of n- and p-type Cu_2O thin films.[20,21] Results showed that the passivation significantly increased the photocurrent while decreasing the Cu_2O thin film resistivity.

In this paper, we present junction characteristics of layered structures of both Cu_2O and CuO that were fabricated by using electrodeposition under controlled conditions for obtaining a p-CuO/n-Cu_2O structure. First, the structural and optical properties were investigated for individual films. Then, the structural, optical and electrical properties of the resulting p-CuO/n-Cu_2O solar cell structure were investigated. Subsequently, sulfur treatment and annealing were successfully used for improving the efficiency of Ti/p-CuO/n-Cu_2O/Au solar cells.

© 2015 The Japan Society of Applied Physics

CuO thin films were deposited on Ti substrates that were cleaned with detergent, diluted HNO_3, in an acetone bath and finally, with distilled water. The electrodeposition process was conducted for 30 min in a three-electrode electrochemical cell containing aqueous solutions of a mixture of 3 M lactic acid, 0.45 M cupric sulphate and sodium hydroxide (NaOH), and maintained at 60 °C. During the potentiostatic deposition that was achieved at 850 mV vs SCE, the pH of the electrolyte was adjusted to pH = 11 by adding a 4 M sodium hydroxide solution.

The CuO films were annealed at different temperatures and times in a temperature-controlled furnace. The photocurrent enhancement of as-deposited and annealed CuO films as photocathodes in photo-electrochemical (PEC) solar cells was studied. Optimal annealing temperature and annealing time were 200 °C and 2 h, respectively. Annealing of the CuO samples improved the output photocurrent performance by a factor of ~20, compared with that of non-annealed samples. The heterojunctions fabricated by electrodepositing the Cu_2O thin films on the CuO thin films that were annealed under above-described conditions resulted in the highest-quality photo-response measurements.

For depositing a Cu_2O thin film on CuO, electrodeposition was performed for 20 min in a three-electrode electrochemical cell containing aqueous solutions of a mixture of 0.1 M sodium acetate and 0.01 M cupric acetate, maintained at 55 °C. The electrodeposition process was performed under a potentiostatic condition of −300 mV vs SCE. Optimization of the deposition parameters of the electrolytic bath and annealing temperature was achieved by measuring the photo-activity of the deposited CuO and CuO/Cu_2O films.

During electrodeposition, the deposition times were controlled for obtaining the desired Cu_2O and CuO thin film thicknesses. Film thicknesses were calculated by using Faraday's law and assuming that only single-phase Cu_2O and CuO films were deposited and the densities of Cu_2O and CuO films were equal to the bulk densities, which were 6 and 6.31 g cm^{-3} for Cu_2O and CuO, respectively. The calculated thicknesses of the Cu_2O films deposited at −300 mV vs SCE for 20 min on Cu_2O and of the CuO films that were electrodeposited at 850 mV vs SCE for 30 min on Ti substrates were ~0.5 μm and ~2 μm, respectively.

X-ray diffraction (XRD) measurements were performed by using a Shimadzu XD-D1 X-ray diffractrometer. Figure 1(a) shows the XRD spectra of the CuO films deposited on the Ti substrates. In Fig. 1(a), all diffraction peaks belong to the CuO phase and there are no characteristic peaks related to the impurities such as Cu or Cu_2O. The strong and sharp peaks reveal the good crystalline nature of the deposited films. It can be also noted that the reflection of $(\bar{1}11)$ orientation is stronger. Figure 1(b) shows the XRD spectra of the Cu_2O films deposited on the bare Ti substrates. In Fig. 1(b), all diffraction peaks belong to the Cu_2O phase other than those that belong to the Ti substrate. Figure 1(c) shows the XRD spectra of the CuO/Cu_2O thin film heterostructure, and the XRD peaks corresponding to both the Cu_2O and CuO layers can be seen. The fine peak profiles corresponding to the reflections from the Cu_2O and CuO grains reveal the formation of CuO/Cu_2O heterojunction from good-quality CuO and Cu_2O polycrystalline layers.

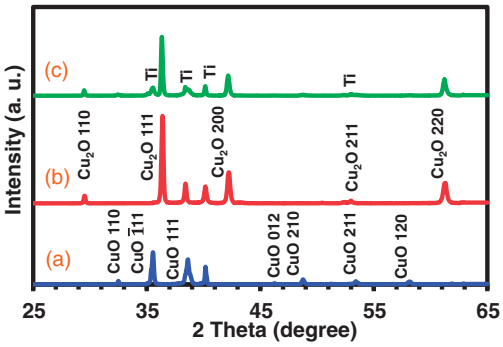

Fig. 1. XRD spectra of (a) a CuO film, (b) a Cu_2O film, and (c) a CuO/Cu_2O heterostructure electrodeposited on a Ti substrate.

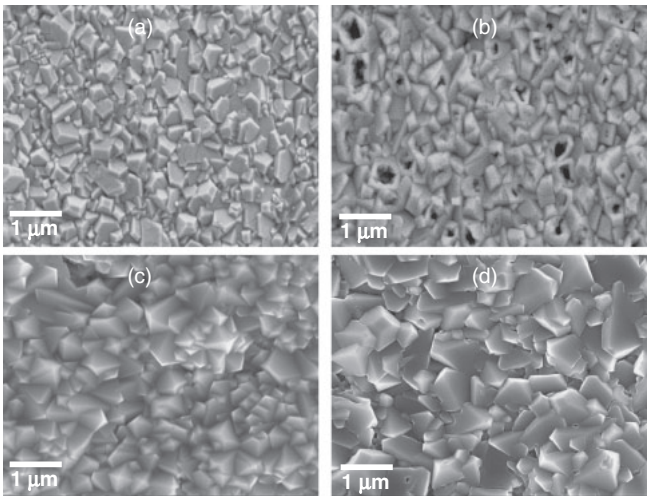

Fig. 2. SEM images of the (a) as-deposited CuO film, (b) CuO film annealed at 200 °C, (c) Cu_2O film on bare Ti substrate, and (d) CuO/Cu_2O heterostructure.

The surface morphology of the films and devices was determined by using a scanning electron microscope (SEM; Philips XL40). Figure 2 shows the SEM images of the as-deposited CuO film on a bare Ti substrate [Fig. 2(a)], the CuO film annealed at 200 °C [Fig. 2(b)], the Cu_2O film on a bare Ti substrate [Fig. 2(c)], and the CuO/Cu_2O heterostructure [Fig. 2(d)]. The prepared films show that the substrate was well-covered with crystals, yielding uniform surface morphology. When the CuO film was annealed at 200 °C [Fig. 2(b)], the grains became much coarser and considerably more porous compared with those in the as-deposited films. The Cu_2O film on the bare Ti substrate grains exhibited 4-sided pyramids with a 4-fold symmetry, with grain sizes of ~0.5 μm. After a layer of Cu_2O was deposited on top of the annealed CuO film, the surface morphology was changed to larger polycrystalline grains having mixed shapes. The Cu_2O crystals grown on the CuO film were larger than those grown on the bare Ti substrate [Figs. 1(c) and 1(d)], which is probably owing to the lower nucleation density and therefore the growth of larger crystals.

To perform the spectral response measurements, all Cu_2O thin films were investigated in a three-electrode photo-electrochemical cell containing 0.1 M sodium acetate solution. The experimental procedure has been discussed in detail elsewhere.[22] Figure 3(a) shows the spectral response characteristics of the CuO and Cu_2O thin film samples, with their

© 2015 The Japan Society of Applied Physics

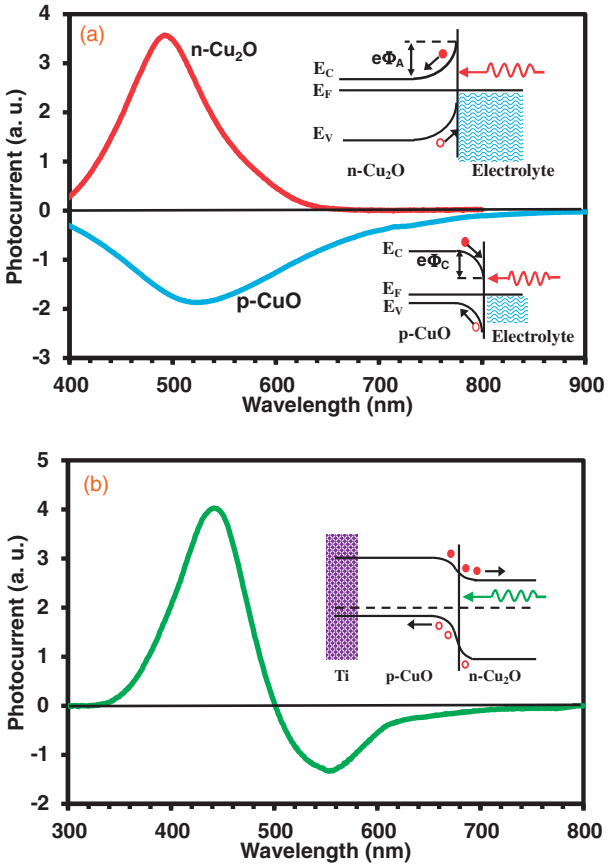

Fig. 3. Spectral responses, measured in the photo-electrochemical cells of (a) CuO and Cu_2O films, and (b) the spectrum of CuO/Cu_2O heterojunction structure with corresponding energy band diagrams.

corresponding energy band diagrams. As shown, a p-type semiconductor has a downward surface band bending and the internal electric field lines in the surface space charge region point from the surface toward the bulk. When the p-type film is irradiated, photo-induced electrons move to the p-type film surface owing to the action of electric field at the surface. On the contrary, for the n-type film with an upward surface band bending, photo-induced holes are driven toward the interface and electrons are driven toward the semiconductor bulk. Therefore, for the two cases the spectral response characteristics exhibit opposite variations, i.e., negative variation for a p-type and positive variation for an n-type film. Negative spectral response implies that the photo-induced electrons move toward the irradiation side of the sample, while positive spectral response implies that the photo-induced holes also move toward the same side.[23] The negative photo-response corresponding to the CuO sample and the positive photo-response corresponding to the Cu_2O samples confirm the p-type conductivity and n-type conductivity of these two sample types, respectively. The spectral response measurements performed for the bare n-Cu_2O thin film showed the onset of photocurrent at ~620 nm, matching the ~2 eV bandgap of Cu_2O, and ~900 nm, matching the ~1.37 eV bandgap of the p-CuO.

Figure 3(b) shows the spectral response for the front-side illuminated CuO/Cu_2O structure (the monochromatic light was irradiated from the surface of the n-Cu_2O side). In general, the absorption coefficient of high energy photons is higher than that of low energy photons, and the photons are absorbed within a short distance from the interface. Therefore, as the photon energy increases the penetration depth of the incident light decreases, and the number of photo-induced excess charge carriers generated at the interface decreases as well. As shown in Fig. 3(b), a positive signal arises when the wavelength of the incident light is shorter than 500 nm ($\lambda < 500$ nm). In contrast, a negative spectral response arises when the wavelength of the incident light is longer than 500 nm ($\lambda > 500$ nm). As a consequence of the separation of photo-induced charge carriers at the junction interface, a net electric field is produced, resulting in an induced photovoltage. The opposite signs of spectral response indicate that there are two transport processes in the film, confirming the existence of the p-CuO/n-Cu_2O heterojunction. It is known that when a p-type semiconductor and an n-type semiconductor come into contact, an interfacial electric field pointing from the n-side to the p-side will be generated. In addition, there is an internal surface space charge layer electric field that exists on the surface of the n-Cu_2O layer. The field is oriented from the bulk toward the surface, opposing the interfacial electric field. When the wavelength of the incident light is longer than 500 nm ($\lambda > 500$ nm), some photons can reach the p-CuO/n-Cu_2O heterojunction. Thus, the entire Cu_2O layer can be excited and photo-induced electrons on the p-CuO side move to the n-Cu_2O side, owing to the interfacial electric field. At the same time, photo-induced holes in the surface space charge region of the n-Cu_2O film move toward the surface of the n-Cu_2O film. However, charge separation at the interface is more effective than that at the surface, owing to relatively stronger interfacial field. In addition, the surface recombination is much higher than the interface recombination, owing to the high concentration of charge carriers on the surface. Therefore, excess photo-induced electrons accumulate at the irradiated n-Cu_2O side and form a negative interface-related spectral response signal. At longer wavelengths, photons may be absorbed in both depletion regions, and charge carriers will be driven in opposite directions. Thus, the net current will be determined by the net effect of the two regions. Direction of the net current flow will be determined by the dominant region, which is the p-CuO/n-Cu_2O junction depletion region. The situation is depicted in Fig. 3(b).

For the surface treatment of the deposited Cu_2O film, the film surface was exposed to 20 vol % $(NH_4)_2S$ solution at 27 °C for about 8 s.[20] Electrical resistivity of the p-CuO/n-Cu_2O films was measured by using the conducting probe technique. Our previous study on n-type Cu_2O showed that increasing the $(NH_4)_2S$ exposure time reduced the film resistivity by several orders of magnitude while remarkably improving the photocurrent.[20] This was attributed to the sulfur passivation that reduced the density of defects arising from non-radiative recombination centers or carrier traps that existed on the surface of the polycrystalline Cu_2O film. In addition, the subsequent formation of the Cu_xS layer on the film surface has given rise to enhanced electrical conductivity.[24] When a similar treatment was used for passivating the thin film/air interface of the n-Cu_2O film of the p-CuO/n-Cu_2O heterojunction, the short circuit photocurrent density increased up to ~6.8 mA cm^{-2} compared with the non-passivated p-CuO/n-Cu_2O heterojunction which yielded a short circuit photocurrent density of ~0.35 mA cm^{-2}. As was

© 2015 The Japan Society of Applied Physics

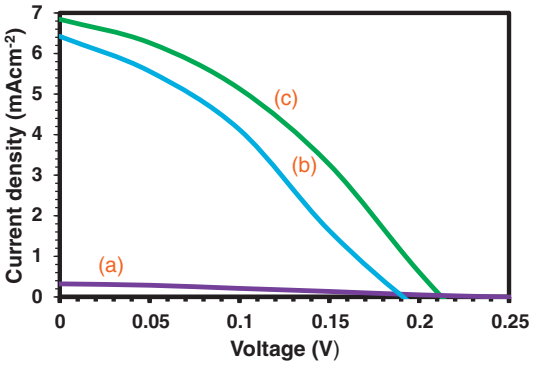

Fig. 4. Current–voltage characteristics of Ti/p-CuO/n-Cu_2O/Au solar cells (a) before sulfur treatment, (b) after sulfur treatment, and (c) after sulfur treatment and annealing at 100 °C for 45 min.

reported previously, the role of the Cu_xS layer that formed upon $(NH_4)_2S$ vapor treatment was twofold. While it minimized the defects on the surface of the n-Cu_2O film for enhancing the conductivity of the n-Cu_2O layer, it also caused the formation of an Ohmic front contact with the Au metal.[20)]

Current–voltage (I–V) measurements were performed by using a Keithley 2100 multimeter. Then, the front ohmic contacts to the films were made by using gold (Au) for fabricating the Ti/p-CuO/n-Cu_2O/Au thin film solar cell structure. For I–V measurements, contacts were made through gold dots placed on the film surface and the Ti substrate.

Figure 4 shows the I–V characteristics of the Ti/p-CuO/n-Cu_2O/Au solar cell device before the sulfur treatment [Fig. 4(a)], after the sulfur treatment [Fig. 4(b)], and after the sulfur treatment and annealing [Fig. 4(c)]. After the ammonium sulfur treatment, the films exhibited enhanced I–V characteristics, owing to reduced resistivity.[20)] The resulting energy conversion efficiency of the sulfur-treated device was 0.52%, with $V_{oc} = 190\,\text{mV}$ and $J_{sc} = 6.4\,\text{mA cm}^{-2}$, obtained under AM 1.5 illumination. Annealing of the sulfur-treated solar cell structures further improved the efficiency, yielding the optimal annealing temperature and annealing time of 100 °C and 45 min, respectively, with energy conversion efficiency of 0.64% with $V_{oc} = 220\,\text{mV}$ and $J_{sc} = 6.8\,\text{mA cm}^{-2}$, whereas the non-annealed non-treated p-Cu_2O layer yielded energy conversion efficiency of 0.03%, with $V_{oc} = 235\,\text{mV}$ and $J_{sc} = 0.35\,\text{mA cm}^{-2}$, obtained under AM 1.5 illumination. Work is still in progress to further improve the efficiency of solar cells by optimizing the deposition parameters, the thickness of semiconducting layers, and the annealing temperature, as well as by using proper Ohmic back contact materials such as Au, Ni.

In conclusion, p-CuO and n-Cu_2O films and p-CuO/n-Cu_2O heterojunction were prepared by using electrodeposition. Results revealed that the efficiency of the solar cell device increased ~20-fold compared with that of the non-treated non-annealed device. The obtained cell yielded the power conversion efficiency of 0.64%, which to the best of our knowledge is the highest reported efficiency for CuO-based solar cells.

Acknowledgment This work was financially supported by the Ministry of Higher Education, Sri Lanka under HETC project through the research grant KLN/O-Sci/N4.

1) B. G. Lewis and D. C. Paine, MRS Bull. **25** [8], 22 (2000).
2) H. Hosono, H. Ohta, K. Hayashi, M. Orita, and M. Hirano, J. Cryst. Growth **237–239**, 496 (2002).
3) A. H. Jayatissa, K. Guo, and A. C. Jayasuriya, Appl. Surf. Sci. **255**, 9474 (2009).
4) Q. Zhang, K. Zhang, D. Xu, G. Yang, H. Huang, F. Nie, C. Liu, and S. Yang, Prog. Mater. Sci. **60**, 208 (2014).
5) I. Y. Y. Bu, Ceram. Int. **39**, 8073 (2013).
6) A. Mittiga, E. Salza, F. Sarto, M. Tucci, and R. Vasanthi, Appl. Phys. Lett. **88**, 163502 (2006).
7) T. Minami, Y. Nishi, and T. Miyata, Appl. Phys. Express **8**, 022301 (2015).
8) Y. F. Lim, J. J. Choi, and T. Hanrath, J. Nanomater. **2012**, 393160 (2012).
9) Q. Bao, C. M. Li, L. Liao, H. Yang, W. Wang, C. Ke, Q. Song, H. Bao, T. Yu, K. P. Loh, and J. Guo, Nanotechnology **20**, 065203 (2009).
10) T. Oku, R. Motoyoshi, K. Fujimoto, T. Akiyama, B. Jeyadevan, and J. Cuya, J. Phys. Chem. Solids **72**, 1206 (2011).
11) K. Fujimoto, T. Oku, T. Akiyama, and A. Suzuki, J. Phys.: Conf. Ser. **433**, 012024 (2013).
12) P. Wang, X. Zhao, and B. Li, Opt. Express **19**, 11271 (2011).
13) F. Gao, X. J. Liu, J. S. Zhang, M. Z. Song, and N. Li, J. Appl. Phys. **111**, 084507 (2012).
14) L. Zhu, J. K. Luo, G. Shao, and W. I. Milne, Sol. Energy Mater. Sol. Cells **111**, 141 (2013).
15) T. Oku, T. Yamada, K. Fujimoto, and T. Akiyama, Coatings **4**, 203 (2014).
16) M. Izaki, T. Shinagawa, K. T. Mizuno, Y. Ida, M. Inaba, and A. Tasaka, J. Phys. D **40**, 3326 (2007).
17) K. Fujimoto, T. Oku, and T. Akiyama, Appl. Phys. Express **6**, 086503 (2013).
18) W. Siripala and J. R. P. Jayakody, Sol. Energy Mater. **14**, 23 (1986).
19) R. P. Wijesundera, M. Hidaka, K. Koga, J. Y. Choi, and N. E. Sung, Ceram.—Silik. **54**, 19 (2010).
20) K. M. D. C. Jayathilaka, V. Kapaklis, W. Siripala, and J. K. D. S. Jayanetti, Phys. Status Solidi: Rapid Res. Lett. **8**, 592 (2014).
21) K. M. D. C. Jayathilaka, V. Kapaklis, W. Siripala, and J. K. D. S. Jayanetti, Electron. Mater. Lett. **10**, 379 (2014).
22) W. Siripala, L. D. R. D. Perera, K. T. L. De Silva, J. K. D. S. Jayanetti, and I. M. Dharmadasa, Sol. Energy Mater. Sol. Cells **44**, 251 (1996).
23) T. P. Hough, *Trends in Solar Energy Research* (Nova Science, New York, 2006) p. 6.
24) A. L. Fahrenbruch and R. H. Bube, *Fundamentals of Solar Cells* (Academic Press, New York, 1983) Chap. 10.

© 2015 The Japan Society of Applied Physics